Ground-state phase diagram of the two-dimensional $t-J$ model

Sheng-Hao Li,[1] Qian-Qian Shi,[1] and Huan-Qiang Zhou[1]

[1]*Centre for Modern Physics and Department of Physics, Chongqing University, Chongqing 400044, The People's Republic of China*

The ground-state phase diagram of the two-dimensional $t-J$ model is investigated in the context of the tensor network algorithm in terms of the graded Projected Entangled-Pair State representation of the ground-state wave functions. There is a line of phase separation between the Heisenberg anti-ferromagnetic state without hole and a hole-rich state. For both $J = 0.4t$ and $J = 0.8t$, a systematic computation is performed to identify all the competing ground states for various dopings. It is found that, besides a possible Nagaoka's ferromagnetic state, the homogeneous regime consists of four different phases: one phase with charge and spin density wave order coexisting with a $p_x(p_y)-$wave superconducting state, one phase with the symmetry mixing of $d+s-$wave superconductivity in the spin-singlet channel and $p_x(p_y)-$wave superconductivity in the spin-triplet channel in the presence of an anti-ferromagnetic background, one superconducting phase with extended $s-$wave symmetry, and one superconducting phase with $p_x(p_y)-$wave symmetry in a ferromagnetic background.

PACS numbers: 74.20.-z, 02.70.-c, 71.10.Fd

Since the discovery of high temperature superconductivity [1], significant progress has been made in our understanding of strong correlation physics. It was Anderson [2] who realized the importance of Mott-Hubbard insulators and put forward the resonating valence bond picture as a promising route towards the understanding of an electron pairing mechanism responsible for an unprecedented high transition temperature, which are observed for copper oxides (cuprates). Actually, the detailed analysis of electronic states deduced from experiments shows that the undoped parent compound is a Mott-Hubbard insulator and the hole doping is mainly on oxygen sites, with its effective low energy physics described by the two-dimensional $t-J$ model [3].

Although a lot of efforts have been made to gain a full picture of the underlying physics of the two-dimensional $t-J$ model (see, e.g., [4–17]), no consensus has been achieved as to the question whether or not the two-dimensional $t-J$ model superconducts. On the one hand, the variational Monte Carlo (VMC) method clearly indicates that the $d_{x^2-y^2}-$wave superconductivity is stable at absolute zero temperature for a physically realistic coupling parameter regime [18], and field theoretical slave-boson approximation yields qualitatively many peculiar phenomenological features of cuprate superconductors [19]. On the other hand, exact diagonalization (ED) of the $t-J$ model on a small cluster and quantum Monte Carlo (QMC) simulation of the two-dimensional Hubbard model do not produce convincing evidence supporting the existence of superconductivity in the $t-J$ model within a physically relevant regime [8, 20].

In this paper, we attempt to investigate the ground-state phase diagram of the two-dimensional $t-J$ model by exploiting a newly-developed tensor network algorithm [21] in terms of the graded Projected Entangled-Pair State (gPEPS) representation of the ground-state wave functions (for an ungraded version, see [22]). It is found that, the algorithm yields reliable results for the two-dimensional $t-J$ model at and away from half filling, with the truncation dimension up to 6. We are able to locate a line of phase separation (PS) between the Heisenberg anti-ferromagnetic state without hole and a hole-rich state, which qualitatively agrees with the results based on the high-temperature expansions (HTE) [11], the VMC [13], and the density-matrix renormalization method (DMRG) [14]. In the homogeneous regime, the two-dimensional $t-J$ model exhibits very rich physics. Away from half filling, the regime is divided into four different phases: one phase with charge and spin density wave order coexisting with a $p_x(p_y)-$wave superconducting state (CDW+SDW+PW), one phase with the symmetry mixing of $d+s-$wave superconductivity in the spin-singlet channel and $p_x(p_y)-$wave superconductivity in the spin-triplet channel in the presence of an anti-ferromagnetic background (DSW+PW+AF), one superconducting phase with extended $s-$wave symmetry (SW), and one superconducting phase with $p_x(p_y)-$wave symmetry in a ferromagnetic background (PW+FM), besides a possible Nagaoka's ferromagnetic state (FM) [23].

Ground-state phase diagram of the two-dimensional $t-J$ model. The two-dimensional $t-J$ model is described by the Hamiltonian [8] consisting of a hopping term and a super-exchange interaction:

$$H = -t\sum_{\langle ij\rangle\sigma}[\mathcal{P}(c^{\dagger}_{i\sigma}c_{j\sigma}+\text{H.c.})\mathcal{P}] + J\sum_{\langle ij\rangle}(\mathbf{S}_i\cdot\mathbf{S}_j-\frac{1}{4}n_i\,n_j), \quad (1)$$

where $\mathbf{S}_i$ are spin $1/2$ operators at site i on a square lattice, $\mathcal{P}$ is the projection operator excluding double occupancy, and t and J are, respectively, the hoping constant and anti-ferromagnetic coupling between the nearest neighbor sites $\langle ij\rangle$.

The model is simulated by exploiting the gPEPS tensor network algorithm [21], with the truncation dimension up to 6. Here, we stress that, although the algorithm is variational in nature, an assumption has to be made on the choice of the unit cell of the gPEPS representation of the ground-state wave functions. For the $t-J$ model, we have chosen the plaquette as the unit cell (see Fig. 1, left panel).

In Fig. 2, we plot the ground-state phase diagram for the two-dimensional $t-J$ model, with the vertical and horizontal axes, n and J/t, denoting the number of electrons per site

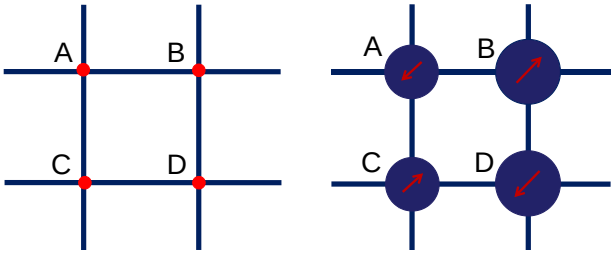

FIG. 1: (color online) Left panel: The unit cell of the graded Projected Entangled-Pair State representation of the ground-state wave functions. Right panel: The pattern of the coexisting charge and spin density wave order. Here, the radius of the circles are proportional to the fillings at sites, whereas the arrows inside the circles represent the directions and magnitudes of the spin density wave order parameters. This represents a vertical commensurate stripe state, which breaks the four-fold rotation symmetry and the translation symmetry in the horizontal direction for charge density wave order and in both directions for spin density wave order.

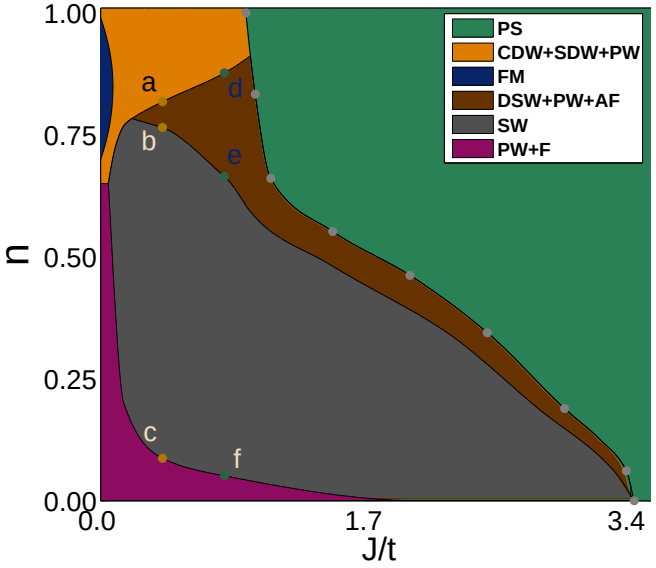

FIG. 2: (color online) The proposed ground-state phase diagram of the two-dimensional $t-J$ model. First, for $J/t \geq 0.95$, there is a line of phase separation (PS), whereas for $J/t \geq 0.95$, no PS occurs. Second, the homogeneous regime is divided into four different phases: one phase with charge and spin density wave order coexisting with a $p_x(p_y)-$wave superconducting state (CDW+SDW+PW), one phase with the symmetry mixing of $d+s-$wave superconductivity in spin-singlet channel and $p_x(p_y)-$wave superconductivity in spin-triplet channel in the presence of an anti-ferromagnetic background (DSW+PW+AF), one superconducting phase with an extended $s-$wave symmetry (SW), and one superconducting phase with a $p-$wave symmetry (PW+F), besides a possible Nagaoka's ferromagnetic state (FM). Here, a systematic computation has been performed for both $J/t = 0.4$ and $J/t = 0.8$ with the truncation dimension $\mathbb{D} = 6$, whereas the dash lines separating different phases are a guide for the eyes. For $J/t = 0.4$, the DSW+PW+AF phase occurs for fillings from $n = 0.818$ (denoted as point a) to $n = 0.765$ (denoted as point b), the SW phase occurs for fillings from $n = 0.765$ to $n = 0.087$ (denoted as point c), and the CDW+SDW+PW and PW+FM phases occur for fillings from $n = 1$ to $n = 0.818$ and from $n = 0.087$ to $n = 0$, respectively. For $J/t = 0.8$, the DSW+PW+AF phase occurs for fillings from $n = 0.877$ (denoted as point d) to $n = 0.665$ (denoted as point e), the SW phase occurs for fillings from $n = 0.665$ to $n = 0.051$ (denoted as point f), and the CDW+SDW+PW and PW+FM phases occur for fillings from $n = 1$ to $n = 0.877$ and from $n = 0.051$ to $n = 0$, respectively.

and the ratio between the anti-ferromagnetic coupling and the hoping constant, respectively. At half filling, $n = 1$, the $t-J$ model reduces to the two-dimensional Heisenberg spin $1/2$ model. Therefore, a long range anti-ferromagnetic order exists [24]. In this case, our algorithm yields the ground-state energy per site, $e = -1.1675J$, for the truncation dimension $\mathbb{D} = 4$, and $e = -1.1683J$, for the truncation dimension $\mathbb{D} = 6$. This is comparable to the best QMC simulation result: $e = -1.1694J$ [24, 25], although the anti-ferromagnetic Néel order moment is 0.36 versus 0.31. Away from half filling, the model exhibits quite different behaviors for small and large values of the anti-ferromagnetic coupling J. For $J/t \geq 0.95$, there is a line of PS between the Heisenberg anti-ferromagnetic state without hole and a hole-rich state, whereas for $J/t \leq 0.95$, no PS occurs. This agrees qualitatively with the results based on the HTE [11], the VMC method [13], and the DMRG [14]. Note that our result for the transition point $J_c = 3.45t$ at low electron density is quite close to the exact value $J_c = 3.4367t$ [15]. Here, the simulation has been performed for the truncation dimension $\mathbb{D} = 6$.

We point out that a discrepancy exists concerning the PS boundary of the $t-J$ model. In Ref. [9], a combination of analytic and numerical calculations is used to establish the existence of PS at all super-exchange interaction strengths. Although the simulation based on the Green's function Monte Carlo method supports this scenario [10], many others [11–14] found that the model phase separates only for J/t larger than some finite critical value around $J/t \sim 1$. That is, PS occurs *only* outside the physically realistic parameter region of the $t-J$ model. With the observation that no significant shift with the truncation dimension $\mathbb{D}$ increasing from $\mathbb{D} = 4$ [21] to $\mathbb{D} = 6$ is found, we conclude that *PS does not occur for* $J/t \leq 0.95$.

In the homogeneous regime, the two-dimensional $t-J$ model exhibits very rich physics. Away from half filling, both the $d+s-$wave superconductivity in the spin-singlet channel and the $p_x(p_y)-$wave superconductivity in the spin-triplet channel, and/or charge and spin density wave order, occur in different doping regimes for a fixed J/t. Here, a superconducting state is characterized by a superconducting order parameter $\Delta \equiv \langle\hat{\Delta}\rangle$, with $\hat{\Delta}$ defined as follows: For s-wave, $\hat{\Delta}_s = 1/(4\sqrt{2})\, c^+_{i_x,i_y\uparrow}[c^+_{i_x+1,i_y\downarrow}+c^+_{i_x-1,i_y\downarrow}+c^+_{i_x,i_y+1\downarrow}+c^+_{i_x,i_y-1\downarrow}]-[\uparrow\leftrightarrow\downarrow]$; for d-wave, $\hat{\Delta}_d = 1/(4\sqrt{2})\, c^+_{i_x,i_y\uparrow}[c^+_{i_x+1,i_y\downarrow}+c^+_{i_x-1,i_y\downarrow}-c^+_{i_x,i_y+1\downarrow}-c^+_{i_x,i_y-1\downarrow}]-[\uparrow\leftrightarrow\downarrow]$; for p_x-wave, $\hat{\Delta}_{p_x} = \hat{\Delta}_{p_x+}-\hat{\Delta}_{p_x-}$, with $\hat{\Delta}_{p_x\pm} = 1/2\,\left(c^+_{i_x,i_y\uparrow}c^+_{i_x\pm1,i_y\uparrow}, [c^+_{i_x,i_y\uparrow}c^+_{i_x\pm1,i_y\downarrow}+c^+_{i_x,i_y\downarrow}c^+_{i_x\pm1,i_y\uparrow}]/\sqrt{2}, c^+_{i_x,i_y\downarrow}c^+_{i_x\pm1,i_y\downarrow}\right)$, and a similar definition of $\hat{\Delta}_{p_y}$ for p_y-wave.

Charge and spin density wave order coexisting with a

$p_x(p_y)-$*wave superconducting state.* For a physically realistic super-exchange coupling J and a hopping constant t (such as $J/t = 0.4$), a spin-triplet $p_x(p_y)-$wave superconducting state coexists with charge and spin density wave order for dopings up to around $\delta \sim 0.18$, with $\delta \equiv 1 - n$. The occurrence of such a spin-triplet $p_x(p_y)-$wave superconducting component is unexpected, although this would, in our opinion, have been anticipated from the presence of the Nagaoka's ferromagnetic state [23]. In addition, Dagotto and Riera [8] observed important ferromagnetic and anti-ferromagnetic correlations in this regime from the ED of the $t - J$ model on a small cluster, which may be properly interpreted as the precursor of a spin-triplet $p_x(p_y)-$wave pairing state, coexisting with charge and spin density wave order. Note that the coexisting charge and spin density wave order forms a pattern, as displayed in Fig. 1 (right panel). In this phase, the translational invariance under one-site shifts, and four-fold rotation symmetry, as well as the $U(1)$ symmetry in the charge sector and the $SU(2)$ symmetry in the spin sector, are spontaneously broken.

In Fig. 3, the magnitude of the spin-triplet $p_x(p_y)-$wave superconducting order parameter Δ_p, along with those of the charge and spin density wave order parameters, are plotted for both $J/t = 0.4$ and $J/t = 0.8$, which have been evaluated with the truncation dimension $\mathbb{D} = 6$. In this phase, all the order parameters are evaluated for two sites A and B in the unit cell, with the subscripts A and B as their labels, except for the charge density wave order parameter that is defined as half the difference between the densities at two sites A and B (see Fig. 1, right panel).

The mixing of the spin-singlet $d + s-$wave and spin-triplet $p_x(p_y)-$wave superconductivity in the presence of an anti-ferromagnetic background. As shown in Fig. 2, there is a superconducting phase with mixed spin-singlet $d + s-$wave and spin-triplet $p_x(p_y)-$wave symmetries in the presence of an anti-ferromagnetic background. For $J = 0.4$, it occurs for fillings from $n = 0.818$ to $n = 0.765$. For $J = 0.8$, it occurs for fillings from $n = 0.877$ to $n = 0.665$. In this phase, the translational invariance under one-site shifts, and four-fold rotation symmetry, as well as the $U(1)$ symmetry in the charge sector and the $SU(2)$ symmetry in the spin sector, are spontaneously broken. Note that the d-wave, s-wave and $p_x(p_y)-$wave components are homogeneous.

In Fig. 3, the magnitudes of the $d-$wave, $s-$wave and $p_x(p_y)-$wave order parameters, Δ_d, Δ_s, and Δ_p (upper panel), along with that of the anti-ferromagnetic order parameter (lower panel), are plotted for the $t-J$ model with $J/t = 0.4$ and $J/t = 0.8$ which have been evaluated with the truncation dimension $\mathbb{D} = 6$. One observes that the $d-$wave component Δ_d vanishes at electron fillings n_{c1}: $n_{c1} = 0.765$ and $n_{c2} = 0.818$ for $J/t = 0.4$ and $n_{c1} = 0.665$ and $n_{c2} = 0.877$ for $J/t = 0.8$. We also list the numerical values of the $d-$wave and $s-$wave components, Δ_d and Δ_s, for both $J/t = 0.4$ and $J/t = 0.8$ at different fillings in Table I, together with their ratio Δ_s/Δ_d. The fact that the pairing symmetry (in the spin-singlet channel) is of the $d + s$-wave nature manifests itself in that the ratio Δ_s/Δ_d is always real. On the other hand, the symmetry mixing of the spin-singlet and spin-triplet channels arises from the spin-rotation symmetry breaking: *spin is not a good quantum number*.

J/t	n	Δ_s	Δ_d	Δ_s/Δ_d
0.4	0.768	$0.0107 - 0.0042i$	$-0.0256 + 0.0100i$	-0.416
	0.776	$0.0101 - 0.0040i$	$-0.0261 + 0.0103i$	-0.386
	0.785	$0.0096 - 0.0037i$	$-0.0266 + 0.0103i$	-0.360
	0.794	$0.0091 - 0.0032i$	$-0.0270 + 0.0100i$	-0.336
	0.804	$0.0085 - 0.0033i$	$-0.0270 + 0.0105i$	-0.314
	0.814	$0.0080 - 0.0031i$	$-0.0272 + 0.0106i$	-0.295
0.8	0.720	$0.0147 - 0.0052i$	$-0.0375 + 0.0134i$	-0.391
	0.722	$0.0145 - 0.0053i$	$-0.0378 + 0.0133i$	-0.383
	0.725	$0.0143 - 0.0050i$	$-0.0382 + 0.0133i$	-0.375
	0.741	$0.0129 - 0.0045i$	$-0.0398 + 0.0139i$	-0.325
	0.757	$0.0116 - 0.0046i$	$-0.0401 + 0.0160i$	-0.289
	0.800	$0.0091 - 0.0037i$	$-0.0419 + 0.0168i$	-0.217
	0.811	$0.0085 - 0.0034i$	$-0.0421 + 0.0169i$	-0.203
	0.833	$0.0076 - 0.0030i$	$-0.0422 + 0.0169i$	-0.179
	0.842	$0.0072 - 0.0029i$	$-0.0419 + 0.0168i$	-0.171

TABLE I: The numerical values of the s-wave and d-wave superconducting order parameters, Δ_s and Δ_d, and their ratio Δ_s/Δ_d for both $J/t = 0.4$ and $J/t = 0.8$ at different fillings in the DSW+PW+AF phase.

The spin-singlet superconducting phase with extended $s-$wave symmetry. For a fixed $0.1 < J/t < 0.95$, if one keeps on increasing doping until the $d-$wave component Δ_d vanishes, then *only* an s-wave order parameter Δ_s survives, resulting in a spin-singlet superconducting phase with extended $s-$wave symmetry. For $J/t = 0.4$ and $J/t = 0.8$, the $s-$wave pairing order parameter Δ_s is plotted in Fig. 3. A peculiar feature of the $s-$wave order parameter is that it is almost linearly increasing with increasing doping, until it reaches its maximum, and then it monotonically decreases.

Although this phase is perhaps only of academic interest due to its unphysical nature of large dopings for cuprate superconductors, we believe it is important to clarify its pairing symmetry. Note that a small portion located between $2.0 \leq J/t \leq 3.4367$ has been identified as a spin-singlet superconducting phase with $s-$wave symmetry in Refs. [9, 10, 15, 26].

The spin-triplet superconducting phase with $p_x(p_y)-$wave symmetry in a ferromagnetic background. For large dopings, a spin-triplet superconducting phase with $p_x(p_y)-$wave symmetry in a ferromagnetic background occurs. The existence of such a spin-triplet superconducting phase with $p_x(p_y)-$wave symmetry has been pointed out by Kagan and Rice [26]. Therefore, our simulation results are consistent with their analytical analysis.

In Fig. 3, the magnitude of the spin-triplet $p-$wave order parameter, together with that of the ferromagnetic order parameter, are plotted for both $J/t = 0.4$ and $J/t = 0.8$ with the truncation dimension $\mathbb{D} = 6$. Here, the $p_x(p_y)-$wave order parameter is identical at all sites, thus it is homogeneous.

Doping-induced quantum phase transitions. Now we turn to doping-induced quantum phase transitions (QPTs) for the

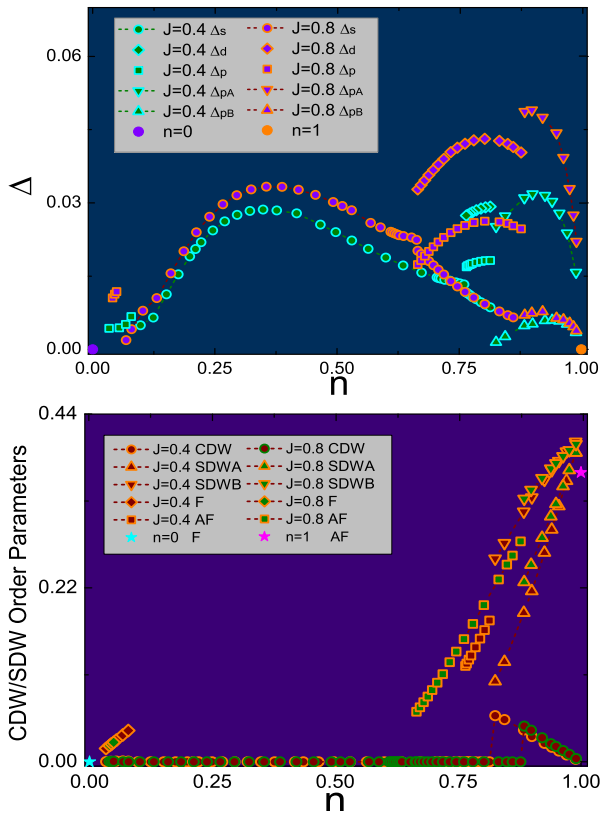

FIG. 3: (color online) Upper panel: The dependence of the d-wave, s-wave, and $p_x(p_y)-$wave superconducting order parameters, Δ_d, Δ_s and Δ_p, on electron filling n. Here, we evaluate Δ_s, Δ_d and Δ_p for $J/t = 0.4$ and $J/t = 0.8$. Lower panel: The dependence of the spin density wave (SDW) and the charge density wave (CDW) order parameters in the CDW+SDW+PW phase, the anti-ferromagnetic Néel order parameter in the DSW+PW+AF phase, and the ferromagnetic order parameter in the PW+F phase on electron filling n. Note that, in the CDW+SDW+PW phase, all the order parameters are evaluated for two sites A and B in the unit cell, with the subscripts A and B as their labels, except for the charge density wave order parameter that is defined as half the difference between the densities at two sites A and B (see Fig. 1, right panel).

two-dimensional $t-J$ model. For $J/t = 0.4$, the model undergoes a QPT from the CDW+SDW+PW phase to the DSW+PW+AF phase at $n = 0.818$, and a QPT from the DSW+PW+AF phase to the SW phase at $n = 0.765$, and again a QPT from the SW phase to the PW+F phase at $n = 0.087$. For $J/t = 0.8$, the model undergoes a QPT from the CDW+SDW+PW phase to the DSW+PW+AF phase at $n = 0.877$, and a QPT from the DSW+PW+AF phase to the SW phase at $n = 0.665$, and again a QPT from the SW phase to the PW+F phase at $n = 0.051$. In addition, a QPT occurs between the DSW+PW+AF phase and the PW+F phase. Here, all QPTs are first-order, as one may judge from the behaviors of the order parameters shown in Fig. 3. In passing, we point out that the above results have been deduced from the ground-state fidelity approach in the context of tensor network representations [27], with superconducting order parameters being read off from both one-site and two-site reduced density matrices according to a general scheme advocated in Ref. [28].

In summary, we have investigated the ground-state phase diagram of the two-dimensional $t-J$ model in the context of the tensor network algorithm. The relevance of our simulation results to the high temperature cuprate superconductors will be discussed in a forthcoming publication [29].

This work is supported in part by the National Natural Science Foundation of China (Grant Nos: 10774197 and 10874252).

[1] J.G. Bednorz and K.A. Müller, Z. Phys. B **64**, 189 (1986).
[2] P.W. Anderson, Science **235**, 1196 (1987).
[3] F.C. Zhang and T.M. Rice, Phys. Rev. B **37**, 3759 (1988).
[4] G. Baskaran and P.W. Anderson, Phys. Rev. B **37**, 580 (1988).
[5] G. Baskaran, Z. Zou, and P.W. Anderson, Solid State Comm. **63**, 973 (1987).
[6] I. Affleck and J.B. Marston, Phys. Rev. B **37**, 3774 (1988).
[7] F.C. Zhang, C. Gros, T.M. Rice, and H. Shiba, Supercond. Sci. Tech. **1**, 36 (1988).
[8] E. Dagotto and J. Riera, Phys. Rev. Lett. **70**, 682 (1993); for a review, see, E. Dagotto, Rev. Mod. Phys. **66**, 763 (1994).
[9] V.J. Emery, S.A. Kivelson, and H.Q. Lin, Phys. Rev. Lett. **64**, 475 (1990).
[10] C.S. Hellberg and E. Manousakis, Phys. Rev. Lett. **78**, 4609 (1997).
[11] W.O. Putikka, M.U. Luchini, and T.M. Rice, Phys. Rev. Lett. **68**, 538 (1992); E. Dagotto, J. Riera, Y.C. Chen, A. Moreo, A. Nazarenko, F. Alcaraz, and F. Ortolani, Phys. Rev. B **49**, 3548 (1994).
[12] H. Fehske, V. Waas, H. Röder, and H. Bütner, Phys. Rev. B **44**, 8473 (1991); D. Poilblanc, Phys. Rev. B **52**, 9201 (1995); M. Kohno, Phys. Rev. B **55**, 1435 (1997).
[13] R. Valenti and C. Gros, Phys. Rev. Lett. 68, 2402 (1992); H. Yokoyama and M. Ogata, J. Phys. Soc. Japan **65**, 3615 (1996); A. Himeda and M. Ogata, Phys. Rev. B **60**, R9935 (1999).
[14] S.R. White and D.J. Scalapino, Phys. Rev. B **61**, 6320 (2000).
[15] C.S. Hellberg and E. Manousakis, Phys. Rev. B **52**, 4639 (1995).
[16] X.G. Wen and P.A. Lee, Phys. Rev. Lett. **76**, 503 (1996).
[17] S. Sorella, G.B. Martins, F. Becca, C. Gazza, L. Capriotti, A. Porolla and E. Dagotto, Phys. Rev. Lett. **88**, 117002 (2002).
[18] For a recent review, see M. Ogata and H. Fukuyama, Rep. Prog. Phys. **71**, 036501 (2008).
[19] For a review, see P. A. Lee, N. Nagaosa, and X.-G. Wen, Rev. Mod. Phys. **78**, 17 (2006).
[20] S. R. White, D. J. Scalapino, R. L. Sugar, E. Y. Loh, J. E. Gubernatis, and R. T. Scalettar, Phys. Rev. B **40**, 506 (1989); E. Dagotto, A. Moreo, F. Ortolani, D. Poilblanc, and J. Riera Phys. Rev. B **45**, 10741 (1992); A. Moreo, Phys. Rev. B **45**, 5059 (1992).
[21] Qian-Qian Shi, Sheng-Hao Li, Jian-Hui Zhao, and Huan-Qiang Zhou, arXiv:0907.5520.
[22] J. Jordan, R. Orús, G. Vidal, F. Verstraete, and J. I. Cirac, Phys. Rev. Lett. **101**, 250602 (2008).
[23] The presence of such a ferromagnetic state is assumed as a result of the variation Monte Carlo method, see H. Yokoyama and H. Shiba, J. Phys. Soc. Japan **56**, 3570 (1987), which is

consistent with the exact result for the motion of one hole in an anti-ferromagnetic background, see, Y. Nagaoka, Phys. Rev. **147**, 392 (1966).
[24] E. Manousakis, Rev. Mod. Phys. **66**, 763 (1994).
[25] D.A. Huse, Phys. Rev. B **37**, 2380 (1988); K.J. Runge, Phys. Rev. B **45**, 12292 (1992); A. W. Sandvik, Phys.Rev. B **56**, 11678 (1997).
[26] M. Yu Kagan and T.M. Rice, J. Phys.: Condens. Matter **6**, 3771 (1994).
[27] H.-Q. Zhou and J.P. Barjaktarevič, J. Phys. A: Math. Theor. **41** 412001 (2008); H.-Q. Zhou, J.-H. Zhao, and B. Li, J. Phys. A: Math. Theor. **41** 492002 (2008); H.-Q. Zhou, R. Orús, and G. Vidal, Phys. Rev. Lett. **100**, 080602 (2008).
[28] H.-Q. Zhou, arXiv:0803.0585.
[29] H.-Q. Zhou, arXiv:1001.3358.